

000 001 002 003 004 005 006 007 008 009 010 HUGME: MULTI-VIEW EMOTION LEARNING ON HET- EROGENEOUS GRAPH

005 **Anonymous authors**

006 Paper under double-blind review

009 ABSTRACT

011 Human emotions are the cornerstone of social interaction. Empowering machine
 012 vision with emotion perception is crucial for building harmonious and empathetic
 013 human-machine collaborative systems across a wide range of domains. Most
 014 mainstream approaches, based on a given image, adhere to the traditional image
 015 content understanding paradigm and conduct end-to-end emotion learning from
 016 the perspective of semantics-emotion association. Despite significant progress,
 017 several challenges remain. From the perspective of visual information repres-
 018 entation, existing methods mostly adhere to the traditional image content semantics
 019 understanding paradigm and conduct end-to-end emotion learning from the per-
 020 spective of content semantics-emotion semantics association, neglecting the rep-
 021 resentation and utilization of the rich structural information inherent in images.
 022 From the perspective of label information representation, existing methods mostly
 023 either directly map and classify visual features using a one-hot labeling approach,
 024 resulting in human emotion labels being treated as meaningless label indices; or
 025 they simply establish single associations between emotion labels. The heteroge-
 026 neous association patterns inherent in complex human emotions have been largely
 027 unexplored. To this end, in this paper, we propose a novel **HugMe** model by
 028 Multi-view emotion learning on Heterogeneous graph. Specifically, for visual
 029 feature learning, we first develop a multi-view emotion representation method to
 030 leverage rich visual features from the perspectives of both semantics and struc-
 031 tures. For label feature learning, we propose a heterogeneous emotion graph rep-
 032 resentation approach, which leverages heterogeneous graph to model the complex
 033 and diverse association patterns between different emotional labels. Finally, we
 034 develop a multi-view emotion classification module to better recognize different
 035 emotions for the given person in the image. In addition to the traditional classi-
 036 fication loss function, to better learn and optimize our proposed HugMe, we also
 037 design a double-constraint loss function to supervise the label learning process.
 038 Extensive experiment results on well-studied human emotion benchmark datasets
 039 demonstrate the superiority and rationality of HugMe.

039 1 INTRODUCTION

041 Accurately identifying human emotional states (*e.g.*, happiness or sadness) from visual images is
 042 crucial for fully understanding human intentions. Due to the significant potential in many applica-
 043 tions such as human-computer interaction, healthcare, online education, and digital entertainment, it
 044 has aroused extensive research attention in recent years Ruan et al. (2021). Different from traditional
 045 image recognition tasks (*e.g.*, object recognition, scene categorization), emotion recognition seems
 046 inherently more challenging, because it involves a much higher level of abstraction and subjectivity
 047 in the human recognition process.

048 Over the past few years, impressive progress has been made on human emotion learning. Early ap-
 049 proaches analyzed emotions through faces, gestures, and other human information Fabian Benitez-
 050 Quiroz et al. (2016); Eleftheriadis et al. (2016). With the rise of context learning, more and more re-
 051 searchers have realized the significant role that context plays in understanding human emotions Kosti
 052 et al. (2017b). In recent years, researchers have also come to realize that a single label cannot fully
 053 capture the complexities of human emotion. To this end, some work has investigated multi-label
 emotion recognition Li et al. (2023), while others have attempted to learn the distribution of emo-

054
055
056
057
058
059
060
061
062
063
064
065
066
067
068
069
070
071
072
073
074
075
076
077
078
079
080
081
082
083
084
085
086
087
088
089
090
091
092
093
094
095
096
097
098
099
100
101
102
103
104
105
106
107
tion labels from continuous dimensions Xu et al. (2025). Although remarkable progress has been accomplished with these efforts, there still remain several limitations to be resolved.

From the perspective of visual information representation, existing methods mostly adhere to the traditional image content semantics understanding paradigm and conduct end-to-end emotion learning from the perspective of *semantics-emotion* association, neglecting the representation and utilization of the rich structural information inherent in images.

From the perspective of label information representation, existing methods mostly either directly map and classify visual features using a one-hot labeling approach, resulting in human emotion labels being treated as meaningless label indices; or they simply establish single associations between emotion labels. The heterogeneous association patterns inherent in complex human emotions have been largely unexplored.

To this end, in this paper, we propose a novel **HugMe** model by Multi-view emotion learning on Heterogeneous graph. Specifically, for visual feature learning, we first develop a multi-view emotion representation method to leverage rich visual features from the perspectives of both semantics and structures. For label feature learning, we propose a heterogeneous emotion graph representation approach, which leverages heterogeneous graph to model the complex and diverse association patterns between different emotional labels. Finally, we develop a multi-view emotion classification module to better recognize different emotions for the given person in the image. In addition to the traditional classification loss function, to better learn and optimize our proposed HugMe, we also design a double-constraint loss function to supervise the label learning process.

Our main contributions can be summarized as follows:

- We propose a MVER method, which leverages rich visual features from the perspectives of both semantics and structures.
- We develop a HEGR approach, which utilizes heterogeneous graph to model the complex and diverse association patterns between different emotional labels.
- To better optimize our proposed HugMe, we design a double-constraint loss function to supervise the label learning process in addition to the classification loss.
- Extensive experiment results on well-studied human emotion benchmark datasets demonstrate the superiority and rationality of HugMe.

2 RELATED WORK

Over the past few years, impressive progress has been made on human emotion learning. Early approaches analyzed emotions through action units, facial expressions, body gestures, or other human information Fabian Benitez-Quiroz et al. (2016); Eleftheriadis et al. (2016).

With the rise of context learning, more and more researchers have realized the significant role that context plays in understanding human emotions. Kosti et al. (2017a) provided a good start to infer human emotion by incorporating the context. They jointly analyzed the person and the whole scene. Lee et al. (2019) presented CAER-Net, which exploits not only human facial expression but also context information in a joint and boosting manner. Motivated by Frege’s Context Principle Resnik (1967) from psychology, Mittal et al. (2020) combined three interpretations of context for emotion recognition, including multiple modalities, background context and social-dynamic context. Shen et al. (2025) exploited a multi-level context feature refinement method for emotion recognition to mitigate the impact caused by conflicting results from multi-level context.

In recent years, researchers have also come to realize that a single label cannot fully capture the complexities of human emotion. To this end, some work has investigated multi-label emotion recognition. Ruan et al. (2020) modeled the inner connections among emotion labels based on an encoder-decoder framework, and treated the multi-label classification task as a sequence generation problem. Inspired by the progress of Graph Convolutional Networks (GCN) in multi-label object detection tasks Chen et al. (2019), Li et al. (2023) proposed to model the emotion label dependency in real-world images with an emotion graph. Wu et al. (2024) studied hierarchical emotion recognition with scene graphs.

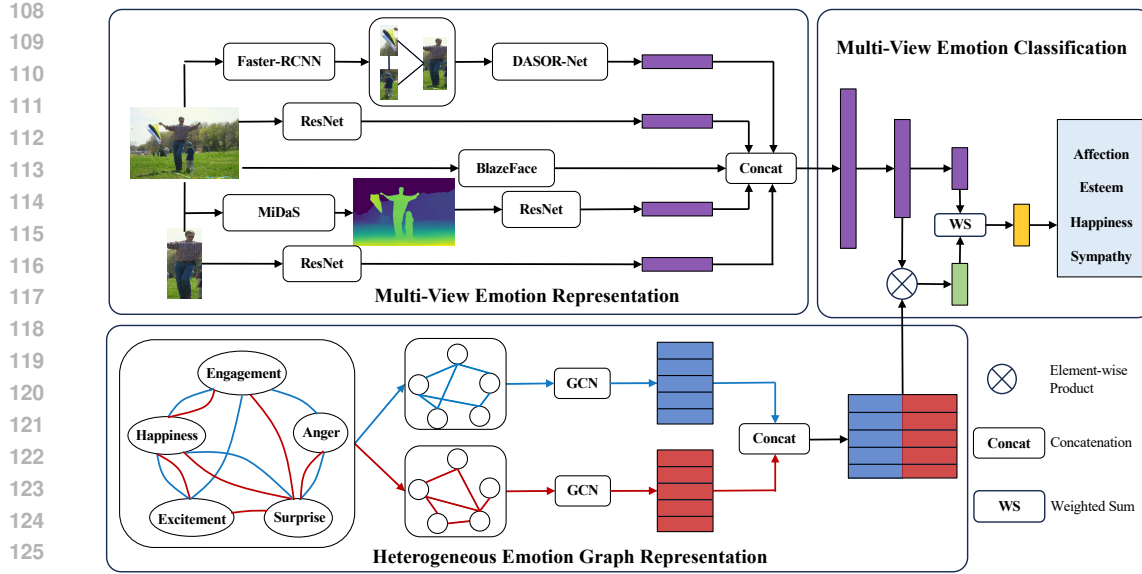


Figure 1: Overall architecture of our proposed HugMe.

Others have attempted to learn the distribution of emotion labels from continuous dimensions. Yang et al. (2021) proposed a well-grounded circular-structured representation to utilize the prior knowledge for visual emotion distribution learning. Further, Yang et al. (2022) developed a novel subjectivity appraise-and-match network (SAMNet) to investigate the subjectivity in visual emotion distribution. From the perspective of information filtering, Xu et al. (2025) proposed a multiple feature refining network to minimize low-level feature redundancy and ensure the purity of emotional information in high-level features.

3 METHOD

The overall architecture of our proposed HugMe is shown in Figure. 1, which consists of three main components. 1) Multi-View Emotion Representation (MVER): representing visual emotion features for both subject persons and context information from different views; 2) Heterogeneous Emotion Graph Learning (HEGL): learning emotional label embedding on a heterogeneous graph by considering both label co-occurrence and semantics similarity; 3) Multi-View Emotion Classification (MVEC): recognizing emotions from different label utilization views.

3.1 MULTI-VIEW EMOTION REPRESENTATION

For the subject person I_s , we employ ResNet He et al. (2016) pre-trained on a web-derived large-scale dataset (*i.e.*, StockEmotion Wei et al. (2020)) to extract subject body features, which can be formulated as follows:

$$f_s = \text{ResNet}(I_s). \quad (1)$$

In addition, we also extract facial (or head) features as a supplement to body features with Blaze-Face Bazarevsky et al. (2019), which is denoted as f_h .

For image context, comprehensive understanding and representation of context play a vital role in human emotion recognition. In this paper, we make full utilization of context information from both semantic and structural views. Moreover, we represent visual emotion features from the views of both global image and local objects. Specifically, we first employ a pre-trained FasterRCNN Ren et al. (2015) to detect the objects around the subject in the image, which is formulated as:

$$l, b = \text{FasterRCNN}(I_{mask}), \quad (2)$$

162 where I_{mask} represents the subject-masked image. $\mathbf{l} \in \mathcal{R}^k$ denotes the detected k object labels.
 163 $\mathbf{b} \in \mathcal{R}^{k \times 4}$ means coordinates of k detected object bounding box.
 164

165 As stated above, both semantic and structural information are important for emotion analysis. There-
 166 fore, we propose a Distance-Aware Relation Network (DARN) to further represent features of local
 167 objects. For object semantics, we consider both visual features and category features, which are
 168 represented as follows:

$$\mathbf{F}_o = [\text{ResNet}(I, \mathbf{b}); \text{emb}(\mathbf{l})]. \quad (3)$$

170 Here, we use $\text{ResNet}(I, \mathbf{b})$ to denote the visual feature matrix of detected object regions, and $\text{emb}(\mathbf{l})$
 171 to represent the object label embedding. \mathbf{F}_o is the extracted object semantic features. The subject-
 172 object distance information is computed as follows:
 173

$$\begin{aligned} 174 \quad dist(\mathbf{b}_s, \mathbf{b}_o) &= \sqrt{(b_s[0] - b_o[0])^2 + (b_s[1] - b_o[1])^2}, \\ 175 \quad \alpha &= \text{softmax}\left(\frac{1}{dist(\mathbf{b}_s, \mathbf{b}_o)}\right), \mathbf{f}_o = \sum_{i=1}^k \mathbf{F}_{oi} \cdot \alpha_i. \end{aligned} \quad (4)$$

179 Here, \mathbf{f}_o is the distance-aware local object feature. $\alpha \in \mathcal{R}^k$ is the calculated relative importance
 180 weight of different objects based on distance perception. $dist(\mathbf{b}_s, \mathbf{b}_o) \in \mathcal{R}^k$ denotes the distance
 181 between the subject person and each object around.
 182

183 For the global context, we employ MiDasRanftl et al. (2020) and ResNet to extract structural depth
 184 information and semantic features of the whole image, which can be formulated as:
 185

$$\mathbf{f}_d = \text{MiDas}(I), \mathbf{f}_g = \text{ResNet}(I). \quad (5)$$

187 Then, we concatenate the above context features and subject person features to comprehensively
 188 represent the image emotion features, which are represented as follows:
 189

$$\mathbf{f}_I = \text{concat}(\mathbf{f}_s; \mathbf{f}_h; \mathbf{f}_o; \mathbf{f}_d; \mathbf{f}_g). \quad (6)$$

193 3.2 HETEROGENEOUS EMOTION GRAPH LEARNING

195 As stated above, there obviously exist correlations among different emotional labels. For example,
 196 ‘happiness’ usually has a larger probability to co-occur with ‘affection’ than ‘anger’. Therefore,
 197 how to model such label dependencies and learn label representations to boost the performance of
 198 emotion recognition is a very critical challenge in our work. In this paper, we propose a Heteroge-
 199 neous Emotion Graph Learning (HEGL) method to model label dependencies.

200 To be specific, for graph nodes, emotional labels are viewed as different nodes in the graph. We
 201 adopt the definition of emotional labels described in Kosti et al. (2017a), and employ a pretrained
 202 BERT Kenton & Toutanova (2019) to extract the semantics representation of label description to ini-
 203 tialize the label embedding, *i.e.*, graph node embedding. We denote the initialized node embedding
 204 as $\mathbf{H}^{(0)}$. In this way, richer emotional semantics of labels can be obtained.

205 For graph edges, as shown in Equation (7), we need to construct the correlation matrix \mathbf{A} . In
 206 the emotional label graph, there are two different types of edges. Therefore, the emotional label
 207 graph is actually a heterogeneous graph. For one type, we compute the cosine similarities among
 208 label embeddings to generate the correlation matrix. For the other type, we also benefit from prior
 209 learning. As suggested by Chen et al. (2019), we model the label correlations with conditional
 210 probability. We use $P(L_j | L_i)$ to denote the probability of occurrence of L_j when L_i appears. To be
 211 specific, we count the occurrence of label pairs in the training set and get the matrix as $\mathbf{O} \in \mathbb{R}^{N \times N}$,
 212 where O_{ij} means the co-occurrence times of label L_i and label L_j . N is the emotional class number.
 213 Then, we also count the occurrence times for each label in the training set, and get the vector as
 214 $\mathbf{m} \in \mathbb{R}^N$. The correlation matrices are computed as follows:
 215

$$A_{ij}^h = \text{Relu}[\cos(\mathbf{H}_i^{(0)}, \mathbf{H}_j^{(0)})], A_{ij}^o = O_{ij} / m_i, \quad (7)$$

216 where A^h and A^o represent the view of similarity and the view of co-occurrence, respectively. Then,
 217 emotional embedding can be updated as follows:

$$\begin{aligned} 218 \quad \mathbf{H}^{h(l+1)} &= \sigma(\widehat{\mathbf{A}}^h \mathbf{H}^{h(l)} \mathbf{W}^{h(l)}), \widehat{\mathbf{A}}^h = \widetilde{\mathbf{D}}^{h^{-\frac{1}{2}}} \mathbf{A} \widetilde{\mathbf{D}}^{h^{-\frac{1}{2}}}, \widetilde{D}_{ii}^h = \sum_j A_{ij}^h, \\ 219 \quad \mathbf{H}^{o(l+1)} &= \sigma(\widehat{\mathbf{A}}^o \mathbf{H}^{o(l)} \mathbf{W}^{o(l)}), \widehat{\mathbf{A}}^o = \widetilde{\mathbf{D}}^{o^{-\frac{1}{2}}} \mathbf{A}^o \widetilde{\mathbf{D}}^{o^{-\frac{1}{2}}}, \widetilde{D}_{ii}^o = \sum_j A_{ij}^o, \\ 220 \quad & \\ 221 \quad & \\ 222 \quad & \\ 223 \quad & \end{aligned} \quad (8)$$

224 where $\mathbf{W}^{(l)}$ is a transformation matrix to be learned. $\widehat{\mathbf{A}}$ is the normalized version of the correlation
 225 matrix \mathbf{A} . $\sigma(\cdot)$ stands for non-linear activation function, i.e., *Relu*.

226 To incorporate them to make the correlation information more comprehensive, we concatenate the
 227 learned label embeddings as follows:

$$228 \quad \mathbf{H} = \text{concat}(\mathbf{H}^{h(l+1)}, \mathbf{H}^{o(l+1)}). \quad (9) \\ 229$$

230 3.3 MULTI-VIEW EMOTION CLASSIFICATION

232 For multi-class or multi-label classification work, previous methods generally have two processing
 233 methods. One is to treat each label as a meaningless one-hot vector form, and they directly map
 234 the image features to the probability distribution of the label category, which lacks the use of the
 235 rich semantic information contained in the label, especially label dependencies; the other is treating
 236 labels as embedding vectors with semantic information, they directly perform label classification
 237 by performing a dot product operation on image features and label embeddings to find similarity.
 238 However, this may introduce uncontrollable noise information due to insufficient label embedding
 239 learning. To this end, in this paper, we develop a Multi-View Emotion Classification (MVEC)
 240 method to make full utilization of label information for better emotion recognition from the two
 241 views.

242 Specifically, as shown in Figure 1, for the first view, we employ a multi-layer perceptron (MLP) to
 243 calculate the distribution probability over all emotional labels. Each MLP has two hidden layers
 244 with *Relu* activation and a *softmax* output layer, which can be formulated as follows:

$$245 \quad \mathbf{p}_1 = \text{MLP}(\mathbf{f}_I), \quad (10)$$

246 where $\mathbf{p}_1 \in \mathcal{R}^n$. For the other view, we use a project layer to transform the image feature into the
 247 same space with the label embedding space, then compute the dot product between image features
 248 and each label embedding. The process can be represented as follows:

$$249 \quad \mathbf{f}'_I = \text{fc}(\mathbf{f}_I), \mathbf{p}_2 = \mathbf{f}'_I \mathbf{H}. \quad (11) \\ 250$$

251 Then, we fuse the results from two different views by weighted sum as follows:

$$252 \quad \mathbf{p} = \beta \mathbf{p}_1 + (1 - \beta) \mathbf{p}_2, \quad (12)$$

253 where \mathbf{p} is the predicted probability across all emotional labels. $\beta \in [0, 1]$ is a hyperparameter.

255 3.4 OBJECTIVE FUNCTION

257 We carefully design the loss function in this paper to better learn and optimize our proposed HugMe
 258 model. To start with common practice, we adopt cross-entropy loss for the classification task as L_C .

259 In HEGR module, we learn better label embeddings by modeling label dependencies. However, the
 260 learning process does not include explicit labels, which may introduce uncertainty noise. There-
 261 fore, we propose a double-constraint loss function to supervise the label-learning process, which is
 262 formulated as follows:

$$\begin{aligned} 263 \quad S_{ij}^o &= \frac{H_i^{o(l+1)} \cdot H_j^{o(l+1)}}{\|H_i^{o(l+1)}\|_2 \cdot \|H_j^{o(l+1)}\|_2}, S_{ij}^h = \frac{H_i^{h(l+1)} \cdot H_j^{h(l+1)}}{\|H_i^{h(l+1)}\|_2 \cdot \|H_j^{h(l+1)}\|_2}, \\ 264 \quad & \\ 265 \quad L_{sem} &= \frac{1}{N^2} \sum_{i=1}^N \sum_{j=1}^N (S_{ij}^h - A_{ij}^h)^2, L_{occur} = \frac{1}{N^2} \sum_{i=1}^N \sum_{j=1}^N (S_{ij}^o - A_{ij}^o)^2, \\ 266 \quad & \\ 267 \quad L_{DC} &= \frac{1}{2} (L_{sem} + L_{occur}), \\ 268 \quad & \\ 269 \quad & \end{aligned} \quad (13)$$

270 where $\|\cdot\|$ is the L_2 norm. L_{sem} and L_{occur} are computed label constraint loss from the perspective
 271 of semantics and cooccurrence, respectively. Then, we average them to obtain the double-constraint
 272 label learning loss L_{DC} . The final objective function of the whole model learning is composed of
 273 the aforementioned terms, which can be formulated as follows:

$$274 \quad 275 \quad L = \lambda L_C + (1 - \lambda) L_{DC}, \quad (14)$$

276 where λ is a hyperparameter ranging from $[0, 1]$ to balance the weight of label classification loss and
 277 label learning loss.

279 4 EXPERIMENT

282 In this section, we first introduce the experiment setup. Then, we evaluate the model performance
 283 on public available dataset. Next, we give detailed analyses and discussions of the model and exper-
 284 imental results.

285 4.1 EXPERIMENT SETUP

288 **Dataset.** To demonstrate the effectiveness of our proposed method, we conduct extensive exper-
 289 iments on the EMOTIC Kosti et al. (2017a) and CAER-S Lee et al. (2019) datasets, following
 290 previous work Zhang et al. (2019); Wu et al. (2024). EMOTIC is a collection of images of people
 291 in unconstrained environments annotated according to their apparent emotional states. It has a total
 292 size of 23,517 images annotated with 26 categories, some of which were manually collected from
 293 Web. Others are from COCO Lin et al. (2014) and Ade20k Zhou et al. (2019). CAER-S has a total
 294 size of 70k images, which are obtained from TV shows. Every image in CAER-S was annotated
 295 by the annotators with a consistent label from seven basic emotion categories, including Anger,
 296 Disgust, Fear, Happy, Sad, Surprise, and Neutral. We follow the data split as the original official
 297 datasets.

298 **Evaluation Metrics and Baselines.** Following Wu et al. (2024), we adopt Average Precision (AP ,
 299 area under the Precision-Recall curves) and mean AP (mAP) scores as evaluation metrics on
 300 EMOTIC dataset. And use *Accuracy* score for evaluation on CAER-S dataset. For a comprehen-
 301 sive comparison, we adopt both small models designed for emotion learning, *e.g.*, Kosti et al.
 302 (2017a); Zhang et al. (2019); Li et al. (2023); Wu et al. (2024) and multi-modal large language
 303 models (MLLM), *e.g.*, BLIP2-6.7b, LLaVa-1.6-7b, GPT-4o and Qwen2.5VL-7B-Instruct as baselines.

304 **Implementation Details.** For model setting, the whole image is resized to 224×224 , while the
 305 head, body, and object region are resized to 128×128 . The dimensions of visual embedding with
 306 ResNet-50, object label embedding, initial emotional label embedding, and emotional label embed-
 307 ding learned from GNN are set as $(2048, 300, 300, 512)$, respectively. λ and β are finally set as 0.8
 308 and 0.5, respectively. For training setting, we use AdamW as optimizer with the initial learning rate
 309 of $1e - 4$, and weight decay of $2.5e - 4$ to mitigate model overfitting. Maximum training epochs
 310 on EMOTIC and CAER-S are set as 50 and 140, respectively. The batch size is set as 60 for both
 311 datasets. During training, we adopt an early stopping strategy and the Optuna tool to help train the
 312 best model.

314 4.2 OVERALL PERFORMANCE

316 In this subsection, we evaluate different models on EMOTIC and CAER-S datasets. As illustrated
 317 in Table 1 and Table 2, our proposed HugMe model achieves the best performance compared with
 318 baseline methods.

319 Among these baselines, Kosti et al. (2017b) and Zhang et al. (2019) make efforts on improving visual
 320 feature representation, while overlook the inherent dependencies among different emotional labels.
 321 To this end, Li et al. (2023) propose to model label relations through an emotion graph, and Wu et al.
 322 (2024) introduce a scene graph for further enhancement. Despite the progress, these methods still
 323 have limitations in mining heterogeneous association patterns (*e.g.*, similarity and cooccurrence)
 among emotional labels.

324

325

Table 1: Overall Performance (AP Scores, %) on EMOTIC Dataset.

Categories	Kosti et al. (2017b)	Zhang et al. (2019)	Li et al. (2023)	Wu et al. (2024)	BLIP2-6.7b	LLaVa-1.6-7b	GPT-4o	QWEN-7b	Ours
Affection	11.29	46.89	18.00	32.25	24.25	34.32	22.53	16.58	25.37
Anger	26.01	10.87	31.52	10.37	8.30	4.98	10.32	32.23	39.21
Annoyance	16.39	11.23	18.53	12.84	8.99	12.37	9.98	7.13	22.04
Anticipation	58.99	62.64	57.30	56.83	91.35	91.87	54.16	54.82	58.08
Aversion	9.56	5.93	6.60	7.70	6.45	6.46	3.51	5.21	9.42
Confidence	81.09	72.49	76.20	77.51	59.37	62.05	68.09	54.47	77.41
Disapproval	16.28	11.28	16.80	12.47	7.56	10.38	8.64	7.92	20.53
Disconnection	21.25	26.91	27.48	26.41	25.85	31.05	17.03	21.73	26.91
Disquietment	20.13	16.94	20.87	16.75	13.53	14.45	17.17	16.35	21.35
Doubt	33.57	18.68	21.04	18.62	18.58	19.06	31.20	17.83	21.48
Embarrassment	3.08	1.94	2.03	2.80	5.45	5.44	2.17	2.02	2.56
Engagement	86.27	88.56	86.14	86.83	95.14	96.10	80.77	79.51	88.05
Esteem	18.58	13.33	14.73	15.50	23.19	23.27	18.30	15.63	15.87
Excitement	78.54	71.89	70.04	70.73	64.51	70.36	69.59	58.37	71.62
Fatigue	10.31	13.26	14.36	12.64	7.68	11.03	9.53	13.18	17.08
Fear	16.44	4.21	6.49	5.48	7.84	8.49	12.79	6.29	9.97
Happiness	55.21	73.26	73.04	69.45	70.77	75.14	53.65	65.49	77.09
Pain	10.00	6.52	9.60	10.64	5.52	5.81	7.45	3.88	12.70
Peace	22.94	32.85	25.24	24.63	20.32	21.26	28.91	16.51	26.54
Pleasure	48.65	57.46	46.96	44.33	43.30	43.49	42.86	31.97	49.34
Sadness	19.29	25.42	30.80	21.21	7.06	18.72	10.70	16.66	36.69
Sensitivity	8.94	5.99	10.01	5.89	4.77	4.75	3.96	2.98	13.95
Suffering	17.60	23.39	29.88	21.48	5.22	6.17	9.74	9.48	36.72
Surprise	21.96	9.02	7.92	7.94	15.42	16.14	17.66	7.36	12.05
Sympathy	15.25	17.53	14.44	13.24	21.48	21.62	9.10	12.48	17.09
Yearning	9.01	10.55	8.78	9.12	13.05	12.79	7.93	6.89	9.15
mAP	28.33	28.42	28.64	26.68	25.96	27.99	23.80	22.42	31.47

351

352

Table 2: Overall Performance on CAER-S Dataset.

Model	Accuracy	Model	Accuracy
Zhao et al. (2021b)	85.87%	BLIP2-6.7b	14.21%
Zhao et al. (2021a)	88.42%	LLaVa-1.6-7b	28.59%
Li et al. (2023)	84.42%	GPT-4o	29.33%
Wu et al. (2024)	90.83%	QWEN-7b	22.42%
Ours	91.11%		

359

360

361

The superiority of our proposed HugMe mainly lies in two aspects. For visual representation, we propose a MVER method to leverages rich visual features from the perspectives of both semantics and structures. For label representation, we develop a HEGR approach, which utilizes heterogeneous graph to model the complex and diverse association patterns between different emotional labels. As shown in Table 1 and Table 2, our proposed HugMe also outperforms MM-LLM based methods, which again demonstrate the effectiveness and superiority of HugMe.

368

369

4.3 ABLATION PERFORMANCE

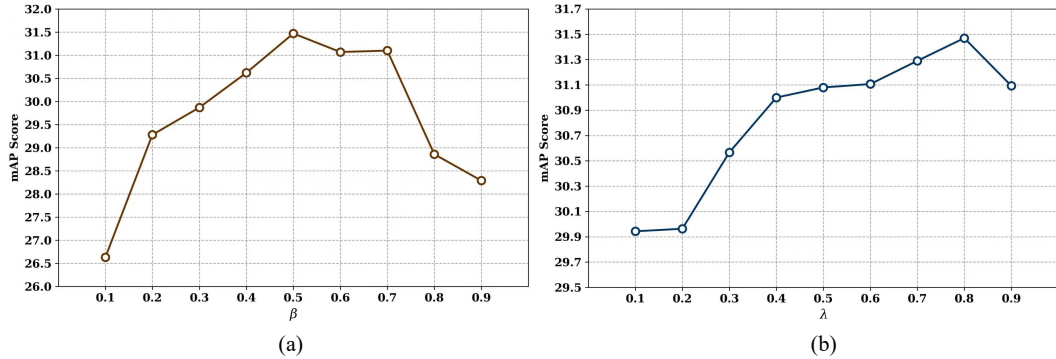
370

The overall experimental results have already proven the superiority of our proposed HugMe method. However, which component is really important for performance improvement is still unclear. Thus, in this subsection, we conduct an ablation study on HugMe to examine the effectiveness of each component. The results are illustrated in Table 3. From the view of information utilization, it is obvious that the performance significantly decreased when removing any information from HugMe separately, which means these information are critical for human emotion learning. From the view of model design, when removing DARN and HEGR separately, experiment results in Table 3 again show the rationality of our proposed method.

378

379
380
Table 3: Ablation Performance (AP Scores, %) of HugMe on EMOTIC Dataset. Here, w/o means
without.

Categories	w/o object	w/o context	w/o head	w/o depth	w/o body	w/o coocurrence	w/o similarity	w/o DARN	w/o HEGR	HugMe
Affection	24.74	19.46	24.82	23.41	24.46	20.89	18.15	22.03	23.85	25.37
Anger	38.84	36.01	40.44	38.95	38.77	38.77	37.03	40.27	38.53	39.21
Annoyance	21.86	19.92	22.26	21.32	21.78	22.25	21.82	21.14	21.06	22.04
Anticipation	57.4	55.69	57.13	57.29	56.75	57.5	57.4	56.94	56.93	58.08
Aversion	9.2	8.12	9.02	9.15	8.82	9.24	9.51	9.36	8.41	9.42
Confidence	76.61	73.09	76.29	76.85	76.11	76.85	76.22	76.87	76.12	77.41
Disapproval	20.24	18.77	20.11	20.28	19.7	20.52	19.38	20.18	18.56	20.53
Disconnection	25.81	24.24	25.5	25.39	25.24	26.23	25.88	24.67	26.7	26.91
Disquietment	20.87	19.68	21.85	19.28	20.11	20.68	21.32	21.19	18.95	21.35
Doubt	21.31	20.56	21.65	21.29	20.84	20.95	22.06	20.82	19.94	21.48
Embarrassment	2.27	2.77	2.4	2.18	2.12	2.26	2.53	2.51	2.42	2.56
Engagement	87.1	86.25	86.68	86.37	87.03	87.28	87.44	87.05	86.77	88.05
Esteem	15.6	15.66	15.48	16.47	16.17	15.88	15.1	15.45	15.62	15.87
Excitement	70.52	68.44	70.53	70.09	69.48	70.39	69.77	70.57	70.61	71.62
Fatigue	17.47	15.56	16.34	17.66	17.61	16.93	15.54	16.28	17.49	17.08
Fear	10.28	7.64	9.13	8.61	9.16	7.89	7.69	8.39	7.75	9.97
Happiness	74.68	74.75	75.81	74.48	73.41	76.38	78.29	77.21	75.46	77.09
Pain	12.01	12.23	12.18	12.6	11.98	11.54	9.64	12.56	10.8	12.70
Peace	26.65	23.47	26.95	26.85	26.45	25.92	23.84	26.75	25	26.54
Pleasure	48.85	48.48	48.5	48.06	47.7	49.38	50.53	49.73	47.5	49.34
Sadness	34.09	30.67	37.05	33.26	34.35	34.35	35.57	35.9	33.51	36.69
Sensitivity	12.28	12.02	11.8	11.75	13.17	12.52	11.49	12.6	11.58	13.95
Suffering	35.04	31.82	34.5	31.88	34.3	33.88	36.39	36.49	34.23	36.72
Surprise	13.11	11.12	13.32	11.72	11.39	10.51	10.29	10.94	10.82	12.05
Sympathy	17.55	15.22	15.54	15.94	16.81	16.22	15.45	14.31	16.79	17.07
Yearning	9.65	9.03	8.78	9.54	9.54	8.96	8.66	8.97	8.33	9.15
mAP	30.92	29.26	30.93	30.41	30.48	30.55	30.27	30.74	30.14	31.47

419
420
Figure 2: Parameter sensitivity study of HugMe on EMOTIC dataset with different settings of β and
421
 λ .422
423
4.4 SENSITIVITY ANALYSIS424
425
As mentioned before, the parameter β and λ control the fusion manner of the final prediction and
426
427
428
429
430
431
432
433
434
435
436
437
438
439
440
441
442
443
444
445
446
447
448
449
450
451
452
453
454
455
456
457
458
459
460
461
462
463
464
465
466
467
468
469
470
471
472
473
474
475
476
477
478
479
480
481
482
483
484
485
486
487
488
489
490
491
492
493
494
495
496
497
498
499
500
501
502
503
504
505
506
507
508
509
510
511
512
513
514
515
516
517
518
519
520
521
522
523
524
525
526
527
528
529
530
531
532
533
534
535
536
537
538
539
540
541
542
543
544
545
546
547
548
549
550
551
552
553
554
555
556
557
558
559
560
561
562
563
564
565
566
567
568
569
570
571
572
573
574
575
576
577
578
579
580
581
582
583
584
585
586
587
588
589
590
591
592
593
594
595
596
597
598
599
600
601
602
603
604
605
606
607
608
609
610
611
612
613
614
615
616
617
618
619
620
621
622
623
624
625
626
627
628
629
630
631
632
633
634
635
636
637
638
639
640
641
642
643
644
645
646
647
648
649
650
651
652
653
654
655
656
657
658
659
660
661
662
663
664
665
666
667
668
669
670
671
672
673
674
675
676
677
678
679
680
681
682
683
684
685
686
687
688
689
690
691
692
693
694
695
696
697
698
699
700
701
702
703
704
705
706
707
708
709
710
711
712
713
714
715
716
717
718
719
720
721
722
723
724
725
726
727
728
729
730
731
732
733
734
735
736
737
738
739
740
741
742
743
744
745
746
747
748
749
750
751
752
753
754
755
756
757
758
759
750
751
752
753
754
755
756
757
758
759
760
761
762
763
764
765
766
767
768
769
770
771
772
773
774
775
776
777
778
779
770
771
772
773
774
775
776
777
778
779
780
781
782
783
784
785
786
787
788
789
780
781
782
783
784
785
786
787
788
789
790
791
792
793
794
795
796
797
798
799
790
791
792
793
794
795
796
797
798
799
800
801
802
803
804
805
806
807
808
809
800
801
802
803
804
805
806
807
808
809
810
811
812
813
814
815
816
817
818
819
810
811
812
813
814
815
816
817
818
819
820
821
822
823
824
825
826
827
828
829
820
821
822
823
824
825
826
827
828
829
830
831
832
833
834
835
836
837
838
839
830
831
832
833
834
835
836
837
838
839
840
841
842
843
844
845
846
847
848
849
840
841
842
843
844
845
846
847
848
849
850
851
852
853
854
855
856
857
858
859
850
851
852
853
854
855
856
857
858
859
860
861
862
863
864
865
866
867
868
869
860
861
862
863
864
865
866
867
868
869
870
871
872
873
874
875
876
877
878
879
870
871
872
873
874
875
876
877
878
879
880
881
882
883
884
885
886
887
888
889
880
881
882
883
884
885
886
887
888
889
890
891
892
893
894
895
896
897
898
890
891
892
893
894
895
896
897
898
899
900
901
902
903
904
905
906
907
908
909
910
911
912
913
914
915
916
917
918
919
920
921
922
923
924
925
926
927
928
929
930
931
932
933
934
935
936
937
938
939
940
941
942
943
944
945
946
947
948
949
950
951
952
953
954
955
956
957
958
959
960
961
962
963
964
965
966
967
968
969
970
971
972
973
974
975
976
977
978
979
980
981
982
983
984
985
986
987
988
989
990
991
992
993
994
995
996
997
998
999
1000
1001
1002
1003
1004
1005
1006
1007
1008
1009
1000
1001
1002
1003
1004
1005
1006
1007
1008
1009
1010
1011
1012
1013
1014
1015
1016
1017
1018
1019
1010
1011
1012
1013
1014
1015
1016
1017
1018
1019
1020
1021
1022
1023
1024
1025
1026
1027
1028
1029
1020
1021
1022
1023
1024
1025
1026
1027
1028
1029
1030
1031
1032
1033
1034
1035
1036
1037
1038
1039
1030
1031
1032
1033
1034
1035
1036
1037
1038
1039
1040
1041
1042
1043
1044
1045
1046
1047
1048
1049
1040
1041
1042
1043
1044
1045
1046
1047
1048
1049
1050
1051
1052
1053
1054
1055
1056
1057
1058
1059
1050
1051
1052
1053
1054
1055
1056
1057
1058
1059
1060
1061
1062
1063
1064
1065
1066
1067
1068
1069
1060
1061
1062
1063
1064
1065
1066
1067
1068
1069
1070
1071
1072
1073
1074
1075
1076
1077
1078
1079
1070
1071
1072
1073
1074
1075
1076
1077
1078
1079
1080
1081
1082
1083
1084
1085
1086
1087
1088
1089
1080
1081
1082
1083
1084
1085
1086
1087
1088
1089
1090
1091
1092
1093
1094
1095
1096
1097
1098
1099
1090
1091
1092
1093
1094
1095
1096
1097
1098
1099
1100
1101
1102
1103
1104
1105
1106
1107
1108
1109
1100
1101
1102
1103
1104
1105
1106
1107
1108
1109
1110
1111
1112
1113
1114
1115
1116
1117
1118
1119
1110
1111
1112
1113
1114
1115
1116
1117
1118
1119
1120
1121
1122
1123
1124
1125
1126
1127
1128
1129
1120
1121
1122
1123
1124
1125
1126
1127
1128
1129
1130
1131
1132
1133
1134
1135
1136
1137
1138
1139
1130
1131
1132
1133
1134
1135
1136
1137
1138
1139
1140
1141
1142
1143
1144
1145
1146
1147
1148
1149
1140
1141
1142
1143
1144
1145
1146
1147
1148
1149
1150
1151
1152
1153
1154
1155
1156
1157
1158
1159
1150
1151
1152
1153
1154
1155
1156
1157
1158
1159
1160
1161
1162
1163
1164
1165
1166
1167
1168
1169
1160
1161
1162
1163
1164
1165
1166
1167
1168
1169
1170
1171
1172
1173
1174
1175
1176
1177
1178
1179
1170
1171
1172
1173
1174
1175
1176
1177
1178
1179
1180
1181
1182
1183
1184
1185
1186
1187
1188
1189
1180
1181
1182
1183
1184
1185
1186
1187
1188
1189
1190
1191
1192
1193
1194
1195
1196
1197
1198
1199
1190
1191
1192
1193
1194
1195
1196
1197
1198
1199
1200
1201
1202
1203
1204
1205
1206
1207
1208
1209
1200
1201
1202
1203
1204
1205
1206
1207
1208
1209
1210
1211
1212
1213
1214
1215
1216
1217
1218
1219
1210
1211
1212
1213
1214
1215
1216
1217
1218
1219
1220
1221
1222
1223
1224
1225
1226
1227
1228
1229
1220
1221
1222
1223
1224
1225
1226
1227
1228
1229
1230
1231
1232
1233
1234
1235
1236
1237
1238
1239
1230
1231
1232
1233
1234
1235
1236
1237
1238
1239
1240
1241
1242
1243
1244
1245
1246
1247
1248
1249
1240
1241
1242
1243
1244
1245
1246
1247
1248
1249
1250
1251
1252
1253
1254
1255
1256
1257
1258
1259
1250
1251
1252
1253
1254
1255
1256
1257
1258
1259
1260
1261
1262
1263
1264
1265
1266
1267
1268
1269
1260
1261
1262
1263
1264
1265
1266
1267
1268
1269
1270
1271
1272
1273
1274
1275
1276
1277
1278
1279
1270
1271
1272
1273
1274
1275
1276
1277
1278
1279<br

432 **5 CONCLUSION**

433

434 Despite the significant progress of existing methods in human emotion recognition, there are still
 435 two main limitations unresolved from the perspectives of both visual information representation and
 436 label information representation. To this end, in this paper, we proposed a novel HugMe model
 437 by multi-view emotion learning on heterogeneous graph. Specifically, we first proposed a MVER
 438 method to leverage rich visual features from the perspectives of both semantics and structures. More-
 439 over, we developed a HEGR approach by utilizing heterogeneous graph to model the complex and
 440 diverse association patterns between different emotional labels. To better optimize our proposed
 441 HugMe, we designed a double-constraint loss function to supervise the label learning process in ad-
 442 dition to the classification loss. Extensive experiment results on benchmark datasets demonstrated
 443 the superiority and rationality of HugMe. Along this line, in the future, we will make efforts to com-
 444 bine the strengths of small models and large models in human emotion learning, from the perspective
 445 of both visual features and label correlations.

446

447 **REFERENCES**

448 Valentin Bazarevsky, Yury Kartynnik, Andrey Vakunov, Karthik Raveendran, and Matthias Grund-
 449 mann. Blazeface: Sub-millisecond neural face detection on mobile gpus. *arXiv preprint*
 450 *arXiv:1907.05047*, 2019.

451

452 Zhao-Min Chen, Xiu-Shen Wei, Peng Wang, and Yanwen Guo. Multi-label image recognition with
 453 graph convolutional networks. In *Proceedings of the IEEE Conference on Computer Vision and*
 454 *Pattern Recognition*, pp. 5177–5186, 2019.

455 Stefanos Eleftheriadis, Ognjen Rudovic, and Maja Pantic. Joint facial action unit detection and
 456 feature fusion: A multi-conditional learning approach. *IEEE transactions on image processing*,
 457 25(12):5727–5742, 2016.

458

459 C Fabian Benitez-Quiroz, Ramprakash Srinivasan, and Aleix M Martinez. Emotionet: An accurate,
 460 real-time algorithm for the automatic annotation of a million facial expressions in the wild. In
 461 *Proceedings of the IEEE conference on computer vision and pattern recognition*, pp. 5562–5570,
 462 2016.

463

464 Kaiming He, Xiangyu Zhang, Shaoqing Ren, and Jian Sun. Deep residual learning for image recog-
 465 nition. In *Proceedings of the IEEE conference on computer vision and pattern recognition*, pp.
 466 770–778, 2016.

467

468 Jacob Devlin Ming-Wei Chang Kenton and Lee Kristina Toutanova. Bert: Pre-training of deep
 469 bidirectional transformers for language understanding. In *Proceedings of NAACL-HLT*, pp. 4171–
 470 4186, 2019.

471

472 Ronak Kosti, Jose M Alvarez, Adria Recasens, and Agata Lapedriza. Emotic: Emotions in context
 473 dataset. In *Proceedings of the IEEE Conference on Computer Vision and Pattern Recognition*
 474 *Workshops*, pp. 61–69, 2017a.

475

476 Ronak Kosti, Jose M Alvarez, Adria Recasens, and Agata Lapedriza. Emotion recognition in con-
 477 text. In *Proceedings of the IEEE conference on computer vision and pattern recognition*, pp.
 478 1667–1675, 2017b.

479

480 Jiyoung Lee, Seungryong Kim, Sunok Kim, Jungin Park, and Kwanghoon Sohn. Context-aware
 481 emotion recognition networks. In *Proceedings of the IEEE International Conference on Computer*
 482 *Vision*, pp. 10143–10152, 2019.

483

484 Weixin Li, Xuan Dong, and Yunhong Wang. Human emotion recognition with relational region-
 485 level analysis. *IEEE Transactions on Affective Computing*, 14(1):650–663, 2023.

486

487 Tsung-Yi Lin, Michael Maire, Serge Belongie, James Hays, Pietro Perona, Deva Ramanan, Piotr
 488 Dollár, and C Lawrence Zitnick. Microsoft coco: Common objects in context. In *European*
 489 *conference on computer vision*, pp. 740–755. Springer, 2014.

486 Trisha Mittal, Pooja Guhan, Uttaran Bhattacharya, Rohan Chandra, Aniket Bera, and Dinesh
 487 Manocha. Emoticon: Context-aware multimodal emotion recognition using frege’s principle.
 488 In *Proceedings of the IEEE/CVF Conference on Computer Vision and Pattern Recognition*, pp.
 489 14234–14243, 2020.

490 René Ranftl, Katrin Lasinger, David Hafner, Konrad Schindler, and Vladlen Koltun. Towards robust
 491 monocular depth estimation: Mixing datasets for zero-shot cross-dataset transfer. *IEEE transac-*
 492 *tions on pattern analysis and machine intelligence*, 44(3):1623–1637, 2020.

493 Shaoqing Ren, Kaiming He, Ross Girshick, and Jian Sun. Faster r-cnn: Towards real-time object
 494 detection with region proposal networks. *Advances in neural information processing systems*, 28,
 495 2015.

496 Michael David Resnik. The context principle in frege’s philosophy. *Philosophy and Phenomeno-*
 497 *logical Research*, 27(3):356–365, 1967. ISSN 00318205. URL <http://www.jstor.org/stable/2106062>.

498 Shulan Ruan, Kun Zhang, Yijun Wang, Hanqing Tao, Weidong He, Guangyi Lv, and Enhong Chen.
 499 Context-aware generation-based net for multi-label visual emotion recognition. In *2020 IEEE*
 500 *International Conference on Multimedia and Expo (ICME)*, pp. 1–6. IEEE, 2020.

501 Shulan Ruan, Kun Zhang, Le Wu, Tong Xu, Qi Liu, and Enhong Chen. Color enhanced cross
 502 correlation net for image sentiment analysis. *IEEE Transactions on Multimedia*, 2021.

503 Xuli Shen, Hua Cai, Weilin Shen, Qing Xu, Dingding Yu, Weifeng Ge, and Xiangyang Xue. Cocoer:
 504 Aligning multi-level feature by competition and coordination for emotion recognition. In *Pro-*
 505 *ceedings of the Computer Vision and Pattern Recognition Conference*, pp. 29591–29600, 2025.

506 Zijun Wei, Jianming Zhang, Zhe Lin, Joon-Young Lee, Niranjan Balasubramanian, Minh Hoai, and
 507 Dimitris Samaras. Learning visual emotion representations from web data. In *Proceedings of the*
 508 *IEEE/CVF Conference on Computer Vision and Pattern Recognition*, pp. 13106–13115, 2020.

509 S Wu, L Zhou, Z Hu, and J Liu. Hierarchical context-based emotion recognition with scene graphs.
 510 *IEEE Transactions on Neural Networks and Learning Systems*, 35(3):3725–3739, 2024.

511 Qinfu Xu, Shaozu Yuan, Yiwei Wei, Jie Wu, Leiquan Wang, and Chunlei Wu. Multiple feature
 512 refining network for visual emotion distribution learning. In *Proceedings of the AAAI Conference*
 513 *on Artificial Intelligence*, volume 39, pp. 8924–8932, 2025.

514 Jingyuan Yang, Jie Li, Leida Li, Xiumei Wang, and Xinbo Gao. A circular-structured represen-
 515 *tation for visual emotion distribution learning*. In *Proceedings of the IEEE/CVF Conference on*
 516 *Computer Vision and Pattern Recognition*, pp. 4237–4246, 2021.

517 Jingyuan Yang, Jie Li, Leida Li, Xiumei Wang, Yuxuan Ding, and Xinbo Gao. Seeking subjectivity
 518 in visual emotion distribution learning. *IEEE Transactions on Image Processing*, 31:5189–5202,
 519 2022.

520 Minghui Zhang, Yumeng Liang, and Huadong Ma. Context-aware affective graph reasoning for
 521 emotion recognition. In *2019 IEEE International Conference on Multimedia and Expo (ICME)*,
 522 pp. 151–156. IEEE, 2019.

523 Zengqun Zhao, Qingshan Liu, and Shanmin Wang. Learning deep global multi-scale and local
 524 attention features for facial expression recognition in the wild. *IEEE Transactions on Image*
 525 *Processing*, 30:6544–6556, 2021a.

526 Zengqun Zhao, Qingshan Liu, and Feng Zhou. Robust lightweight facial expression recognition
 527 network with label distribution training. In *Proceedings of the AAAI conference on artificial*
 528 *intelligence*, volume 35, pp. 3510–3519, 2021b.

529 Bolei Zhou, Hang Zhao, Xavier Puig, Tete Xiao, Sanja Fidler, Adela Barriuso, and Antonio Torralba.
 530 Semantic understanding of scenes through the ade20k dataset. *International Journal of Computer*
 531 *Vision*, 127(3):302–321, 2019.

532